Pathogens and Disease, 2022, **80**, 1–13
DOI: 10.1093/femspd/ftac004
Advance access publication date: 17 January 2022
Research Article

The autophagy-resistant *Mycobacterium tuberculosis* Beijing strain upregulates KatG to evade starvation-induced autophagic restriction

Tegar Adriansyah Putra Siregar[1,2], Pinidphon Prombutara[3,4], Phongthon Kanjanasirirat[5], Nawapol Kunkaew[6], Alisa Tubsuwan[7], Atsadang Boonmee[8], Tanapat Palaga[8], Tanawadee Khumpanied[5], Suparerk Borwornpinyo[5,9], Angkana Chaiprasert[10], Pongsak Utaisincharoen[1] and Marisa Ponpuak[1,11,*]

[1]Department of Microbiology, Faculty of Science, Mahidol University, Rama VI Road, Bangkok 10400, Thailand
[2]Department of Microbiology, Faculty of Science, University of Muhammadiyah Sumatera Utara, Gedung Arca Road, Medan 20217, Indonesia
[3]Omics Sciences and Bioinformatics Center, Faculty of Science, Chulalongkorn University, Phayathai Road, Bangkok 10330, Thailand
[4]Microbiome Research Unit for Probiotics in Food and Cosmetics, Faculty of Science, Chulalongkorn University, Phayathai Road, Bangkok 10330, Thailand
[5]Excellent Center for Drug Discovery, Faculty of Science, Mahidol University, Ratchawithi Road, Bangkok 10400, Thailand
[6]Mahidol Vivax Research Unit, Faculty of Tropical Medicine, Mahidol University, Rama VI Road, Bangkok 10400, Thailand
[7]Institute of Molecular Biosciences, Mahidol University, Phuttamonthon 4 Road, Nakhon Pathom 73170, Thailand
[8]Department of Microbiology, Faculty of Science, Chulalongkorn University, Phayathai Road, Bangkok 10330, Thailand
[9]Department of Biotechnology, Faculty of Science, Mahidol University, Rama VI Road, Bangkok 10400, Thailand
[10]Office of Research and Development, Siriraj Hospital, Faculty of Medicine, Mahidol University, Wanglang Rd, Bangkok 10700, Thailand
[11]Pornchai Matangkasombut Center for Microbial Genomics, Department of Microbiology, Faculty of Science, Mahidol University, Rama VI Road, Bangkok 10400, Thailand
*__Corresponding author:__ Faculty of Science, Department of Microbiology, Mahidol University, Rama VI Road, Bangkok 10400, Thailand. Tel: +02-201-5522; Fax: +02-644-5411; E-mail: marisa.pon@mahidol.ac.th
One sentence summary: A new role of KatG in autophagy evasion by *M. tuberculosis*.
Editor: Andrew Olive

Abstract

Mycobacterium tuberculosis utilizes several mechanisms to block phagosome–lysosome fusion to evade host cell restriction. However, induction of host cell autophagy by starvation was shown to overcome this block, resulting in enhanced lysosomal delivery to mycobacterial phagosomes and the killing of the *M. tuberculosis* reference strain H37Rv. Nevertheless, our previous studies found that strains belonging to the *M. tuberculosis* Beijing genotype can resist starvation-induced autophagic elimination, though the mycobacterial factors involved remain unclear. In this study, we showed that KatG expression is upregulated in the autophagy-resistant *M. tuberculosis* Beijing strain (BJN) during autophagy induction by the starvation of host macrophages, while such increase was not observed in the H37Rv. KatG depletion using the CRISPR-dCas9 interference system in the BJN resulted in increased lysosomal delivery to its phagosome and decreased its survival upon autophagy induction by starvation. As KatG functions by catabolizing ROS, we determined the source of ROS contributing to the starvation-induced autophagic elimination of mycobacteria. Using siRNA-mediated knockdown, we found that Superoxide dismutase 2, which generates mitochondrial ROS but not NADPH oxidase 2, is important for the starvation-induced lysosomal delivery to mycobacterial phagosomes. Taken together, these findings showed that KatG is vital for the BJN to evade starvation-induced autophagic restriction.

Keywords: *Mycobacterium tuberculosis*, tutophagy, tuberculosis, ROS, KatG, CRISPR

Introduction

Tuberculosis caused by the pathogenic bacteria *Mycobacterium tuberculosis* is one of the top 10 leading causes of death among the world population (WHO 2020). The ability of *M. tuberculosis* to survive in host cells stems from its successful deployment of several mechanisms to evade host cell immunity. Among these mechanisms is the inhibition of its phagosome fusion to lysosome (Fratti *et al.* 2001, 2003; Vergne *et al.* 2004). To accomplish this, *M. tuberculosis* utilizes various factors. For example, it has been shown that the mycobacterial glycolipid ManLAM can impair phagosome maturation (Fratti *et al.* 2003). In addition, *M. tuberculosis* secretes the proteins PtpA (Bach *et al.* 2008), SapM (Vergne *et al.* 2005), EsxH (Mehra *et al.* 2013), and CpsA (Koster *et al.* 2017) to block phagolysosome biogenesis. However, the induction of host cell autophagy by cytokine treatment or starvation was recently shown to overcome the phagosome–lysosome arrest, resulting in enhanced lysosomal delivery to mycobacterial phagosomes and the elimination of mycobacteria (Gutierrez *et al.* 2004; Harris *et al.* 2009; Ponpuak *et al.* 2010; Singh *et al.* 2010; Castillo *et al.* 2012; Pilli *et al.* 2012; Haque *et al.* 2015; Chauhan *et al.* 2016).

Autophagy is a conserved eukaryotic lysosomal-dependent degradation process that has multiple effects on innate and adaptive immunity (Deretic *et al.* 2013). It has been shown to play important roles in defending against intracellular bacteria, parasites, and viruses (Deretic and Levine 2009; Deretic *et al.* 2013; Gomes and Dikic 2014; Huang and Brumell 2014). Autophagy of intracel-

Received: September 14, 2021. **Revised:** December 28, 2021. **Accepted:** January 13, 2022

lular pathogens, termed xenophagy, is initiated by a stress signal such as the detection of pathogen-associated molecular patterns by host cells, the presence of host cytokines, and the starvation of the infected cells due to the consumption of host cell amino acids by pathogens (Mizushima *et al.* 2011; Deretic *et al.* 2013; Filomeni *et al.* 2014). During autophagy, double-membrane autophagosomes sequester the pathogens and traffic the microtubules to fuse with lysosomes concentrated in the perinuclear region, resulting in the delivery of lysosomal hydrolases and elimination of the microbes (Yim and Mizushima 2020).

In the context of *M. tuberculosis* infection, induction of autophagy by host cell starvation has been shown to overcome phagosome–lysosome fusion arrest, resulting in the elimination of the *M. tuberculosis* reference strain H37Rv (Gutierrez *et al.* 2004; Harris *et al.* 2009; Ponpuak *et al.* 2010; Singh *et al.* 2010; Castillo *et al.* 2012; Pilli *et al.* 2012; Haque *et al.* 2015; Chauhan *et al.* 2016). However, our previous studies showed that, unlike H37Rv, which was restricted by starvation-induced autophagic control of host macrophages dependent upon the autophagy protein Beclin-1, strains belonging to the notorious Beijing genotype were able to resist starvation-induced autophagic elimination by host cells (Haque *et al.* 2015). Of note, the Beijing genotype was previously shown to have a greater ability to survive inside host macrophages, cause high bacterial load and greater mortality rates in animal models, and have high acid-fast bacilli smear-positive sputum in human patients (Zhang *et al.* 1999; Dormans *et al.* 2004; Tsenova *et al.* 2005; Hanekom *et al.* 2007; van der Spuy *et al.* 2009; Portevin *et al.* 2011). Moreover, we showed that escape of the Beijing strains from starvation-induced autophagic restriction was not simply achieved by inhibiting the autophagy-mediated acidification of their phagosomes or dampening the general autophagic flux in host cells as there was no alteration in the Lysotracker red-mycobacteria colocalization or number of RFP-GFP-LC3^{+} autophagic vacuoles upon autophagy induction by starvation of host cells (Haque *et al.* 2015). However, the Beijing strains were able to evade starvation-induced autophagic elimination by blocking the xenophagic flux (Haque *et al.* 2015). While lysosomes were delivered to the H37Rv phagosomes during starvation-induced autophagy dependent upon Beclin-1, lysosomal delivery to phagosomes of the autophagy-resistant Beijing strain (BJN) was blocked (Haque *et al.* 2015). We also recently showed that, through RNA-Seq analysis of the infected host cells, macrophages infected with the BJN upregulated gene function in lysosome positioning toward cell periphery to facilitate the escape of the BJN from starvation-induced autophagic restriction (Laopanupong *et al.* 2021). However, the mycobacterial factors involved in the autophagy resistance by the BJN remain unknown.

As host cell starvation is known to induce ROS production (Scherz-Shouval *et al.* 2007) and ROS has been shown to be required for efficient autophagosome maturation (Xu *et al.* 2014; An *et al.* 2020), we hypothesized that the BJN may upregulate the expression of the ROS-inhibitory factor to escape from starvation-induced autophagic elimination. Our results showed that KatG was upregulated in the BJN, but not in H37Rv, during autophagy induction by starvation of host macrophages. When KatG was depleted from the BJN, the mycobacteria lost the ability to resist starvation-induced autophagic restriction, as shown by the lowered survival rate in the host macrophages and enhanced lysosomal delivery to its phagosome upon autophagy induction by starvation. The source of ROS contributing to the starvation-induced lysosomal delivery to the mycobacterial phagosomes was determined to be dependent on the Superoxide dismutase 2 (Sod2), which generates mitochondrial ROS, but not the NADPH oxidase 2 (Nox2). Consequently, our results support the role of KatG in the evasion of starvation-induced autophagic control by the BJN.

Materials and methods

Cells and bacterial culture

RAW264.7 macrophages (ATCC) were cultivated in Dulbecco's modified Eagle's medium (DMEM; Gibco) supplemented with 10% fetal bovine serum (FBS; Gibco), 4 mM L-glutamine (Hyclone), and 0.37% sodium bicarbonate (Sigma; full medium) at 37°C and additional 5% CO_2. Earle's Balanced Salt Solution (EBSS; Gibco) was used for autophagy induction (starve medium). Bone marrow-derived macrophages (BMDMs) were isolated from bone marrow cells of C57/BL6 mice (Nomura Siam International, Thailand) using L929 condition media as described elsewhere with modification (Weischenfeldt and Porse 2008) and stored in liqiuid nitrogen until use. All animal procedures were approved by the Institutional Animal Care and Use Committee of Faculty of Medicine, Chulalongkorn University (approval protocol number 025/2562). Cryopreserved BMDMs were then thawed for experiments and cultured in DMEM (Gibco) supplemented with 10% FBS (Gibco), 1% sodium pyruvate (Sigma), 1% HEPES (Gibco), and 20% L929 cell conditioned medium. *Mycobacterium tuberculosis* reference strain H37Rv (ATCC) and the autophagy-resistant Beijing strain (BJN; Haque *et al.* 2015; Laopanupong *et al.* 2021) were propagated in Middlebrook 7H9 broth or on 7H10 agar supplemented with 10% oleic acid–albumin–dextrose–catalase (OADC; BD), 0.05% Tween 80, and 0.2% glycerol at 37°C. Before the experiments, logarithmic phase cultures were collected, washed twice with PBS, and resuspended in the full medium. The log-phase cultures were then homogenized to produce single-cell mycobacteria before measuring the absorbance at 600 nm.

Fluorescent dyes, antibodies, and siRNAs

For immunofluorescence assays, anti-Cathepsin D monoclonal antibody (R&D Systems) and secondary antibodies (Thermo Fisher Scientific) were used at 1:50 and 1:400. For nuclear staining, Hoechst 33342 (Thermo Fisher Scientific) was used at 1:500. For ROS detection, DCFDA (Abcam) was used at 1:800. Alexa 488 and 568 carboxylic acid succinimidyl ester (Invitrogen) were prepared as 1 mg/ml stock solutions and used at 1:100 to label mycobacteria. siRNAs against Nox2 or Sod2 and the scrambled control siRNAs (Dharmacon) were used at 1.5 μg per reaction.

Macrophage infection and RNA isolation

RAW264.7 macrophages were cultured in 75 cm^2 tissue culture flasks at 80% confluence and BMDMs were cultured in non-tissue culture treated petri dishes. Cells were then lifted, plated onto 6-well plates (1×10^6 cells per well), and rested for 16–18 h. Cells were infected with *M. tuberculosis* reference H37Rv or BJN at multiplicity of infection (MOI) of 10 for 2 h. Cells were then washed three times with PBS and subjected to starvation-induced autophagy by EBSS addition for 2 h. For RNA isolation, the media was removed and 0.5 ml of Trizol (Thermo Fisher Scientific) was added to each well and incubated for 5 min at room temperature. Nucleic acids were isolated by bead-beating the samples three times with 0.1 mm zirconia beads (1 min bead-beat and 1 min rest on ice). The supernatants were transferred into nuclease-free microcentrifuge tubes followed by centrifugation at 13 000 rpm for 3 min. Nucleic acids were isolated from the supernatants by the chloroform extraction and isopropanol precipitation (Aiewsakun *et al.* 2021). Turbo DNase (Thermo Fisher Scientific) was added to de-

grade the genomic DNAs. Isolated RNAs were then collected using the RNeasy kit (Qiagen) according to the manufacturer's instructions.

qRT-PCR analysis

A total of 2 μg of total RNAs were used in reverse transcription using random hexamers (Promega), as previously described (Aiewsakun *et al.* 2021). Primers used for the target genes were synthesized by Ward Medic (Table S1, Supporting Information). The converted cDNAs were used as templates for qRT-PCR assays using a thermocycler machine (Rotor-Gene Q, Qiagen) with reactions consisting of HotStarTaq DNA buffer and polymerase (Qiagen), 4 mM $MgCl_2$ (Qiagen), 10 mM dNTPs (Promega), SYBR green (Invitrogen), and 0.1 mM forward and reverse primers at an annealing temperature of 55°C. Reactions-minus templates were used as negative controls. The signals obtained were then analysed using Q-Rex software version 1.0.1. Melting curves were analysed to verify the specificity of the PCR products and the threshold signals were confirmed to be > 95% efficient. Signal values were then normalized to the housekeeping genes *sigA* (for mycobacteria) or *Gapdh* (for host macrophages) and presented as relative quantification using the $2^{-\Delta\Delta ct}$ method.

CRISPR interference system construction and gene expression knockdown

sgRNA targeting *katG* was designed as previously described (Rock *et al.* 2017; Aiewsakun *et al.* 2021). In brief, a 20-bp sequence immediately following the 5′-NNAGAAG-3′ in the *katG* gene was selected. The *katG* specific complementary oligonucleotides with BsmBI restriction sites: katG forward primer 5′-GGGAACCCATGTCGAGCAGGTTCAC-3′ and katG reverse primer 5′-AAACGTGAACCTGCTCGACATGGGT-3′, were commercially synthesized (Ward Medic), then annealed and subcloned into the PLJR965 CRISPRi vector backbone (Rock *et al.* 2017) at BsmBI restriction sites. The insertion of the sgRNA sequence was verified by direct sequencing using the 1834 primer 5′- TTCCTGTGAAGAGCCATTGATAATG-3′. To reduce the expression of *katG*, plasmids containing sgRNA targeting *katG* or non-targeting sgRNA control were then transformed into H37Rv and BJN, as previously described (Goude *et al.* 2015). Transformants were selected on 7H10 agar and maintained in 7H9 medium containing kanamycin (30 μg/ml; Pacific BioLabs). Gene expression was knocked down by Anhydrotetracycline (ATc) induction (100 ng/ml; Sigma) for 4 days, as previously described (Rock *et al.* 2017). RNA isolation and qRT-PCR analysis were conducted, as described above, to determine successful gene expression knockdown.

Mycobacterial survival assay

Mycobacterial survival assay by CFU analysis was performed as previously described (Ponpuak *et al.* 2009). In brief, RAW264.7 macrophages and BMDMs (3×10^5 cells per well) were plated onto 12-well plates and rested for 16–18 h. Cells were then infected with different *M. tuberculosis* strains at MOI of 10 for 1 h, washed three times with PBS to remove the uninternalized mycobacteria, and then induced to undergo autophagy by starvation for 4 h. To harvest the intracellular mycobacteria, cells were lysed by osmotic burst followed by serial dilution and plated onto the 7H10 agars, with or without kanamycin addition (30 μg/ml; Pacific BioLabs). Plates were incubated at 37°C for 2–3 weeks until colonies were visible for counting. Percent mycobacterial survival was then calculated and compared between conditions.

siRNA-mediated knockdown

siRNA-mediated knockdown was performed as previously described (Ponpuak *et al.* 2009). In brief, RAW264.7 macrophages were collected and resuspended in 90 μl of solution V (Lonza). Scramble control siRNAs or siRNAs against Nox2 or Sod2 was added to the cell suspension, transferred to a nucleofection cuvet, and nucleofected using the Amaxa Nucleofector apparatus (Amaxa Biosystems; program D-032). At 24 h post-transfection, cells were collected and plated for assays.

High-content image analysis for Cathepsin D or ROS colocalization with mycobacteria

For colocalization of Cathepsin D, used as a lysosome marker, with mycobacteria, RAW264.7 macrophages and BMDMs were plated onto 96-well black plates (2.5×10^4 cells per well) and then infected with *M. tuberculosis* labelled with Alexa 488 (Ponpuak *et al.* 2009) at MOI of 10 for 15 min. Cells were washed with full medium three times to remove the uninternalized mycobacteria and chased for 1 h (Ponpuak *et al.* 2009). Cells were then washed with PBS three times and induced to undergo autophagy by starvation for 2 h. Cells were fixed with 4% paraformaldehyde and processed for anti-Cathepsin D followed by Alexa 568 secondary antibody staining. Hoechst was used to stain the nucleus. Percent mycobacteria–Cathepsin D colocalization was then analysed by high-content image analysis (Operetta, PerkinElmer).

For the colocalization analysis of ROS with mycobacteria, RAW264.7 macrophages and BMDMs were plated onto 96-well black plates and then infected with *M. tuberculosis* labelled with Alexa 568 at MOI of 10 as described above. After the chase period, cells were subjected to starvation-induced autophagy for 2 h. At 45 min before starvation was completed, DCFDA was added to the cells for ROS staining. Cells were fixed with 4% paraformaldehyde and the nucleus was stained with Hoechst. The samples were then analysed by high-content image analysis. Percent mycobacteria–ROS colocalization was then calculated and compared between conditions.

For colocalization analysis of KatG-deficient or non-targeting sgRNA control mycobacteria with Cathepsin D or ROS, gene expression knockdown was induced with ATc addition for 4 days in 7H9 medium containing kanamycin, as described above. The ATc-induced mycobacteria were then washed with PBS and stained with Alexa 488 or 568 for 1 h, as described above. RAW264.7 cells and BMDMs were then infected with Alexa-labelled KatG-deficient or non-targeting sgRNA control mycobacteria in ATc-containing full medium at MOI of 10 for 15 min, washed with PBS three times, and chased for 1 h in ATc-containing full medium. Cells were then subjected to autophagy induction by starvation for 2 h in ATc-containing EBSS, while the control cells were incubated in ATc-containing full medium. Cells were then fixed and stained for markers, as described above, before being analysed by high-content image analysis.

Statistical analysis

Unless otherwise indicated, all experiments were performed independently at least three times; data were collected and pooled to determine the mean ± standard error of the mean (SEM). All statistics were analysed by Prism software (GraphPad) using a two-tailed unpaired Student's t-test or one-way ANOVA.

Results

KatG is upregulated and required for autophagy resistance by the BJN

Our previous studies showed that, unlike H37Rv, which was restricted by starvation-induced autophagic control of host macrophages, the BJN could resist such elimination and did so by inhibiting lysosomal delivery into its phagosome (Haque *et al.* 2015). However, the mycobacterial factors involved were unclear. As host cell starvation was known to induce ROS production (Scherz-Shouval *et al.* 2007) and ROS was shown to be required for efficient autophagosome maturation (Xu *et al.* 2014; An *et al.* 2020), we hypothesized that the BJN may upregulate the expression of the ROS-neutralizing factor to escape from starvation-induced autophagic elimination. Interestingly, we found that only the BJN significantly increased *katG* expression when RAW264.7 macrophages were infected with H37Rv or BJN and induced to undergo autophagy by starvation, while H37Rv did not (Fig. 1A). Mycobacterial KatG is a catalase–peroxidase that functions in catabolizing ROS generated by host macrophages (Manca *et al.* 1999; Ng *et al.* 2004). As a result, the role of KatG in autophagy evasion by the BJN was examined further.

To determine this, we first confirmed the autophagy resistance phenotype of the BJN. In agreement with our previous data (Haque *et al.* 2015; Laopanupong *et al.* 2021), starvation-induced autophagy of RAW264.7 macrophages resulted in the restriction of *M. tuberculosis* reference strain H37Rv, while the BJN resisted such elimination (Fig. 1B). Similar results were observed in primary BMDMs. When BMDMs were infected with H37Rv or BJN followed by autophagy induction by starvation, only the BJN significantly upregulated *katG* expression but H37Rv did not (Fig. 1C). Moreover, the BJN could escape from starvation-induced autophagic restriction in BMDMs, while H37Rv could not (Fig. 1D). We also confirmed our results using additional autophagy-resistant *M. tuberculosis* Beijing strain (BJY) and autophagy-sensitive East African Indian strain (EAI; Haque *et al.* 2015). The BJY significantly upregulated *katG* expression during starvation-induced autophagy of RAW264.7 macrophages, while such effects were not observed with H37Rv or EAI (Figure S1A, Supporting Information). In agreement with our previous work (Haque *et al.* 2015), the EAI could be restricted by starvation-induced autophagy of Raw264.7 macrophages, while the BJY could resist such control (Figure S1B, Supporting Information).

We then depleted *katG* expression in the H37Rv and BJN using the CRISPR-dCAS9 interference system developed for *M. tuberculosis* (Rock *et al.* 2017). The small-guided RNA (sgRNA) containing *katG* targeting sequence was designed and subcloned into the CRISPR-dCAS9 plasmid (Rock *et al.* 2017), as described in the materials and methods section. The plasmid was then transformed into H37Rv and BJN using the empty vector as the control. Successful knockdown of *katG* mRNA and protein expressions were confirmed in both strains after 4 days of Anhydrotetracycline (ATc) induction as determined by qRT-PCR and immunoblotting (Fig. 1E; Figure S1C–E, Supporting Information). A mycobacterial survival assay upon starvation-induced autophagy was then performed by CFU analysis, as previously described (Ponpuak *et al.* 2009). In agreement with the above results observed with the wild-type mycobacteria, H37Rv carrying the non-targeting sgRNA control could be restricted upon autophagy induction by starvation of RAW264.7 macrophages and BMDMs, while the non-targeting sgRNA control harboring BJN could resist such elimination (Fig. 1F and G). KatG depletion in the BJN, however, reverted such resistance phenotype, resulting in the restriction of the KatG-deficient BJN upon autophagy induction by the starvation of RAW264.7 macrophages and BMDMs (Fig. 1F and G). These data indicated that KatG is required for the BJN to resist starvation-induced autophagic elimination.

Evasion of lysosomal delivery to the BJN phagosome during starvation-induced autophagy depends on KatG

To determine whether the reverted resistance phenotype of the KatG-deficient BJN to starvation-induced autophagic restriction observed above was a result of an increase in lysosomal delivery to the KatG-deficient BJN phagosome, colocalization of the mycobacteria with Cathepsin D, used as a lysosome marker, was examined by high-content image analysis. In agreement with our previous reports (Haque *et al.* 2015; Laopanupong *et al.* 2021), enhanced colocalization of H37Rv with Cathepsin D was observed upon autophagy induction by the starvation of Raw264.7 macrophages, while such effect was not seen with the BJN (Fig. 2A and B). We also confirmed our previous work in which an increased colocalization of the EAI phagosome with Cathepsin D was observed during starvation-induced autophagy of RAW264.7 macrophages but not with that of the BJY (Figure S2A and B, Supporting Information). In addition, consistent with the results seen in RAW264.7 cells, when BMDMs were induced to undergo autophagy by starvation, H37Rv–Cathepsin D colocalization was significantly increased, while such effect was not observed with the BJN (Fig. 3A and B). We, then performed the above experiments using the KatG-deficient mycobacteria. There was a significant increase in colocalization of H37Rv harboring the non-targeting sgRNA control with Cathepsin D upon autophagy induction by starvation of RAW264.7 macrophages and BMDMs, but such change could not be observed with the BJN carrying the non-targeting sgRNA control (Figs 2A, B and 3A, B). However, autophagy induction by starvation of both RAW264.7 macrophages and BMDMs now resulted in significantly enhanced Cathepsin D colocalization with the KatG-deficient BJN phagosome (Figs 2A, B and 3A, B). Altogether, these findings suggested that KatG plays a critical role in suppressing lysosomal delivery to the BJN phagosome during starvation-induced autophagy, and thus spares the BJN from autophagic restriction.

KatG plays a role in reducing ROS associated with the BJN phagosome

Our results showed that the BJN upregulated KatG, which was required for its escape from starvation-induced lysosomal delivery and autophagic restriction. Mycobacterial KatG is known for its function to neutralize ROS generated by host macrophages (Manca *et al.* 1999; Ng *et al.* 2004) and ROS was shown to be required for efficient autophagosome maturation (Xu *et al.* 2014; An *et al.* 2020). Therefore, we set out to determine whether the BJN could alter the level of ROS associated with its phagosome, and thus suppress lysosomal delivery to its compartment during autophagy induction by starvation.

We first confirmed that starvation of host cells resulted in increased ROS production, and such effect was not altered by ATc addition (Figure S3, Supporting Information). To examine whether the BJN could alter the ROS level associated with its phagosome, RAW264.7 macrophages were infected with H37Rv or BJN and then induced to undergo autophagy by starvation. DCFDA was added 45 min before starvation was completed in order to detect ROS. High-content image analysis showed that while there was a significant increase in ROS associated with the H37Rv phagosome

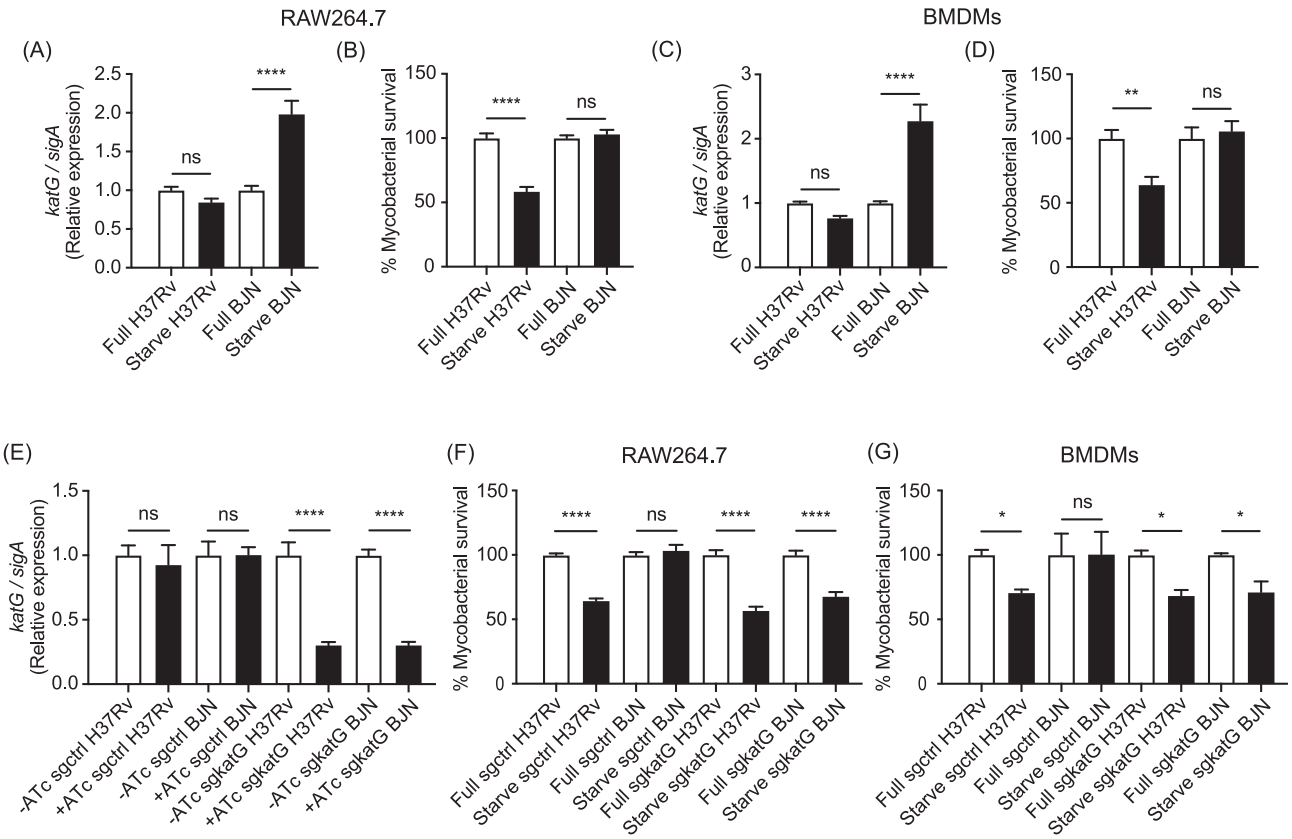

Figure 1. KatG is upregulated and required for the evasion of starvation-induced autophagic control by the BJN. **(A)** RAW264.7 macrophages were infected with *M. tuberculosis* reference strain H37Rv or BJN followed by autophagy induction by starvation for 2 h. Total RNAs were isolated and *katG* expression was quantified by qRT-PCR. Relative gene expression was normalized to the housekeeping gene *sigA* using the $2^{-\Delta\Delta ct}$ method. Data comprise means ± SEM from at least three independent experiments; $^{****}P < .0001$, relative to the full medium control set to 1.0, which was determined by one-way ANOVA with Tukey's multiple comparison test. **(B)** RAW264.7 macrophages were infected with H37Rv or BJN and then induced to undergo autophagy by starvation for 4 h. Intracellular mycobacterial survival was then determined by CFU analysis. Data shown comprises means ± SEM from at least three independent experiments; $^{****}P < .0001$, relative to the full control set to 100%, which was determined by one-way ANOVA with Tukey's multiple comparison test. **(C)** BMDMs were infected with H37Rv or BJN followed by autophagy induction by starvation and *katG* expression was quantified by qRT-PCR as in (A). Data comprise means ± SEM from at least three independent experiments; $^{****}P < .0001$, relative to the full medium control set to 1.0, which was determined by one-way ANOVA with Tukey's multiple comparison test. **(D)** BMDMs were infected with H37Rv or BJN and induced to undergo autophagy by starvation as in (B). Intracellular mycobacterial survival was then determined by CFU analysis. Data shown comprises means ± SEM from at least three independent experiments; $^{**}P < .01$, relative to the full control set to 100%, which was determined by one-way ANOVA with Tukey's multiple comparison test. **(E)** H37Rv or BJN carrying the sgRNA targeting *katG* or the non-targeting sgRNA control plasmid were subjected to Anhydrotetracycline (ATc) induction for 4 days. *katG* expression was then determined by qRT-PCR. Data comprise means ± SEM from at least three independent experiments; $^{****}P < .0001$, all relative to the uninduced control set to 1.0, which was determined by one-way ANOVA with Tukey's multiple comparison test. **(F)** RAW264.7 macrophages were infected with H37Rv or BJN harboring the sgRNA targeting *katG* or the non-targeting sgRNA control plasmid followed by autophagy induction by starvation for 4 h. Intracellular mycobacterial survival was then determined by CFU analysis. Data comprise means ± SEM from at least three independent experiments; $^{****}P < .0001$, relative to the full control set to 100%, which was determined by one-way ANOVA with Tukey's multiple comparison test. **(G)** BMDMs were infected with different *M. tuberculosis* strains and induced to undergo autophagy by starvation as in (F). Intracellular mycobacterial survival was then determined by CFU analysis. Data comprise means ± SEM from at least three independent experiments; $^{*}P < .05$, all relative to the full control set to 100%, which was determined by one-way ANOVA with Tukey's multiple comparison test. Full, macrophages without autophagy induction; starve, macrophages with autophagy induction by starvation; sgctrl, non-targeting sgRNA control; and sgkatG, sgRNA targeting *katG*.

upon autophagy induction by starvation, such effect was not seen with the BJN (Fig. 4A and B). Similar results were also observed when RAW264.7 macrophages were infected with the EAI or BJY and induced to undergo autophagy by starvation. An enhanced colocalization of ROS with the EAI phagosome was detected, while such change was not seen with that of the BJY (Figure S4A and B, Supporting Information). In addition, consistent with the results observed in RAW264.7 macrophages, a significant increase in ROS–H37Rv colocalization was seen in BMDMs during autophagy induction by starvation, but not with that of the BJN (Fig. 5A and B).

Next, we conducted the above experiments using the KatG-deficient H37Rv and BJN. Similar to the results observed with the wild-type mycobacteria, enhanced ROS association with H37Rv harboring the non-targeting sgRNA control was observed during starvation-induced autophagy of RAW264.7 macrophages and BMDMs, while such effects were not seen with that of the BJN harboring the non-targeting sgRNA control (Figs 4A, B and 5A, B). These findings suggested that the BJN could dampen ROS level associated with its phagosome upon autophagy induction by starvation of host cells. However, a significant rise in ROS associated with the KatG-deficient BJN phagosome could be observed when KatG was depleted from the BJN (Figs 4A, B and 5A, B). Altogether, these data suggested that KatG plays a crucial role in reducing ROS associated with the BJN phagosome during the starvation-induced autophagy of host macrophages.

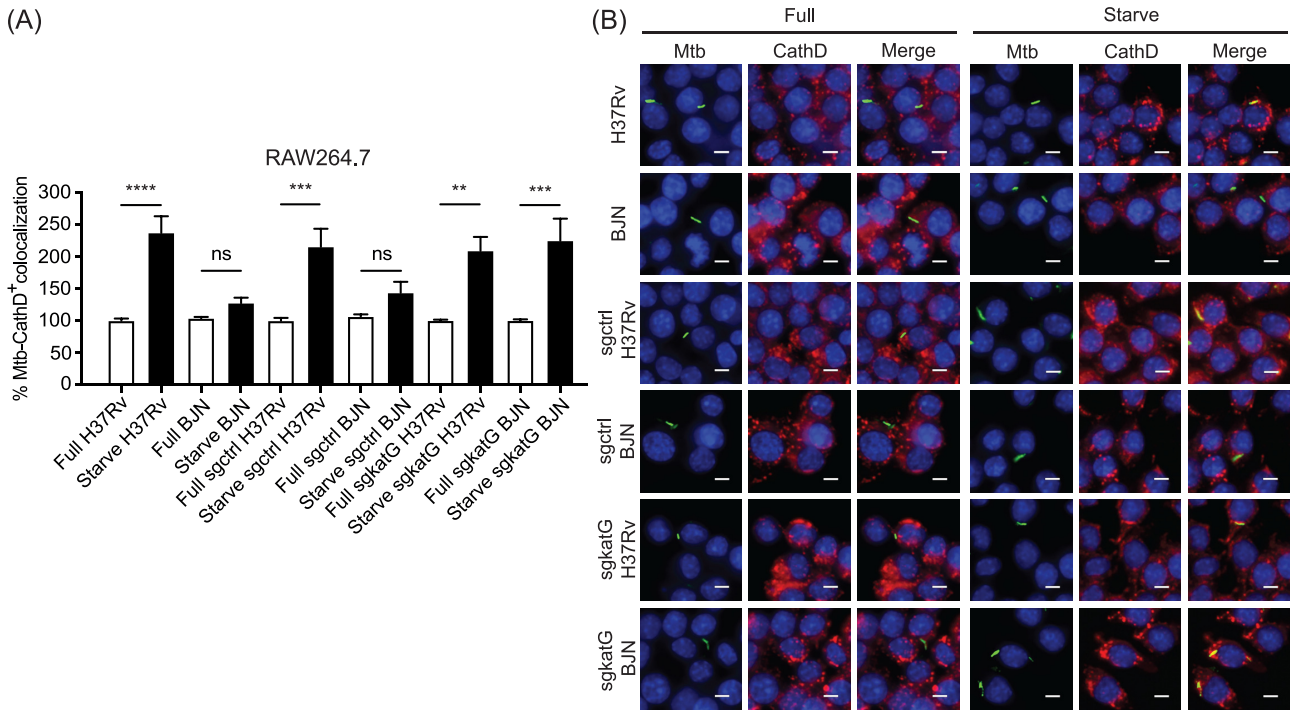

Figure 2. KatG dampens lysosomal delivery to the BJN phagosome in RAW264.7 macrophages during autophagy induction by starvation. **(A)** and **(B)** RAW264.7 macrophages were infected with Alexa-488-labelled H37Rv or BJN for 15 min and chased for 1 h. Host cells were then induced to undergo autophagy by starvation for 2 h. Cells were fixed and stained for Cathepsin D. Mycobacteria–Cathepsin D colocalization was then analysed by high-content image analysis. Data comprise means ± SEM from at least three independent experiments; $^{**}P < .01$, $^{***}P < .001$, and $^{****}P < .0001$, all relative to the full control set to 100%, which were determined by one-way ANOVA with Tukey's multiple comparison test (A). Representative images are shown in (B). Bar 5 μm. Full, macrophages without autophagy induction; starve, macrophages with autophagy induction by starvation; sgctrl, non-targeting sgRNA control; and sgkatG, sgRNA targeting *katG*.

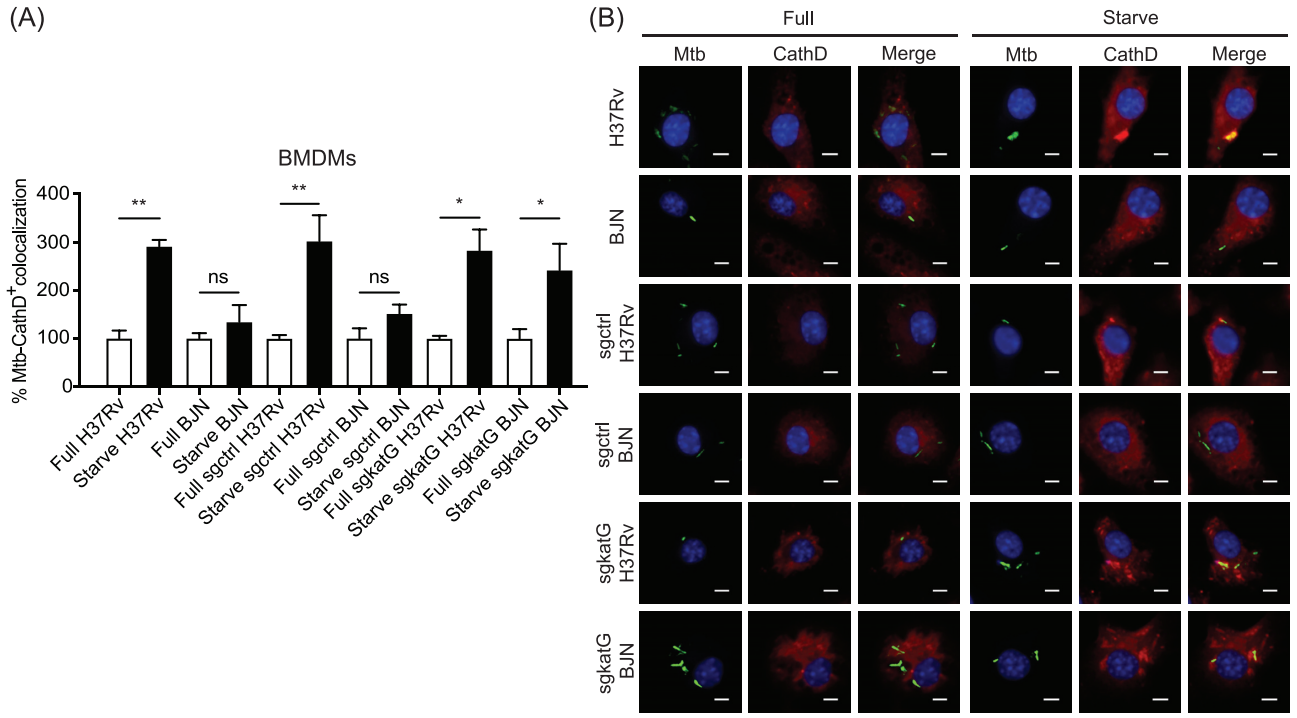

Figure 3. Lysosomal delivery to the BJN phagosome in BMDMs during starvation-induced autophagy is decreased by KatG. **(A)** and **(B)** BMDMs were infected with Alexa-488-labelled H37Rv or BJN for 15 min, chased for 1 h, and induced to undergo autophagy by starvation for 2 h. Cells were fixed and stained for Cathepsin D as in Fig. 2. Mycobacteria–Cathepsin D colocalization was then analysed by high-content image analysis. Data comprise means ± SEM from at least three independent experiments; $^{*}P < .05$ and $^{**}P < .01$, all relative to the full control set to 100%, which were determined by one-way ANOVA with Tukey's multiple comparison test (A). Representative images are shown in (B). Bar 5 μm. Full, macrophages without autophagy induction; starve, macrophages with autophagy induction by starvation; sgctrl, non-targeting sgRNA control; and sgkatG, sgRNA targeting *katG*.

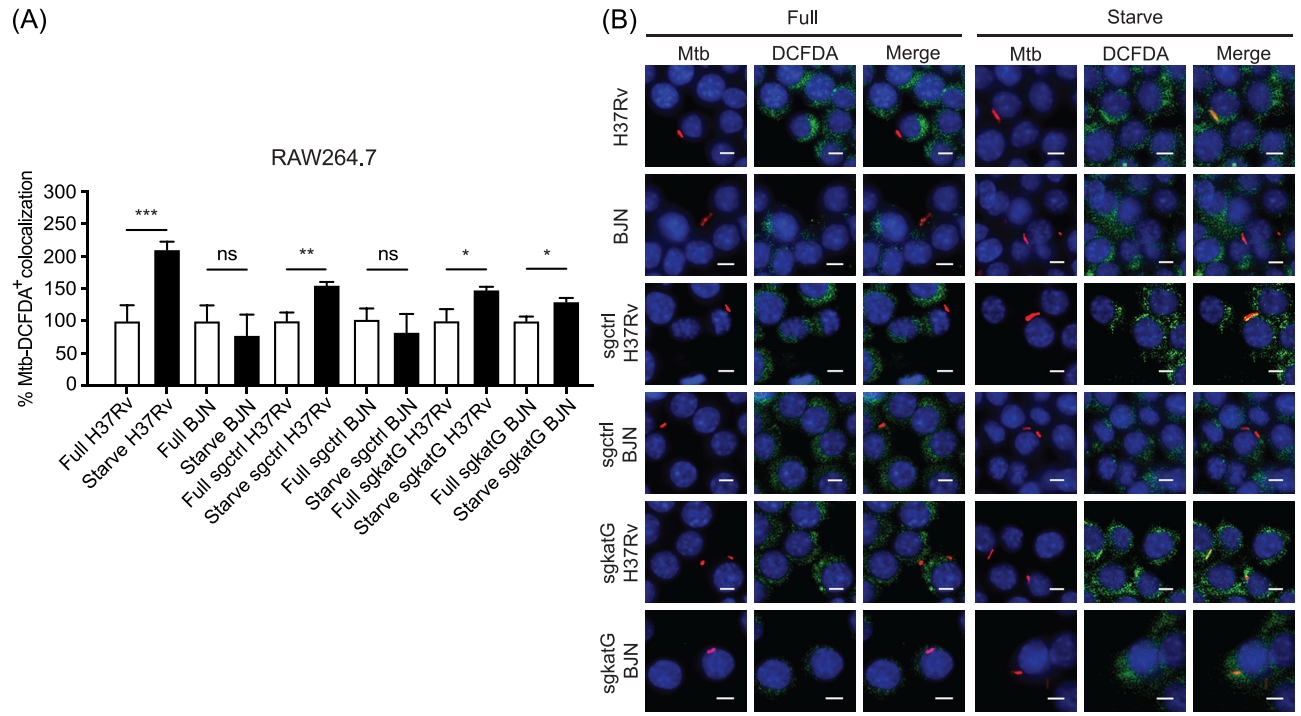

Figure 4. KatG reduces ROS associated with the BJN phagosome in RAW264.7 macrophages during autophagy induction by starvation. **(A)** and **(B)** RAW264.7 macrophages were infected with Alexa-568-labelled H37Rv or BJN strain for 15 min and chased for 1 h. Host cells were then subjected to autophagy induction by starvation for 2 h. A total of 45 min before starvation was completed, cells were stained for ROS using DCFDA. Colocalization of ROS with mycobacteria was then analysed by high-content image analysis. Data comprise means ± SEM from at least three independent experiments; $^{*}P < .05$, $^{**}P < .01$, and $^{***}P < .001$, all relative to the full control set to 100%, which were determined by one-way ANOVA with Tukey's multiple comparison test (A). Representative images are shown in (B). Bar 5 μm. Full, macrophages without autophagy induction; starve, macrophages with autophagy induction by starvation; sgctrl, non-targeting sgRNA control; and sgkatG, sgRNA targeting *katG*.

Sod2-generated ROS is important for starvation-induced lysosomal delivery to mycobacterial phagosomes

In an attempt to determine the source of ROS contributing to the enhanced lysosomal delivery to mycobacterial phagosomes during autophagy induction by starvation, we utilized siRNA knockdown technology to deplete the expression of Nox2 and Sod2 from RAW264.7 macrophages. Nox2 is the catalytic subunit of the NADPH oxidase that functions to generate ROS at the phagosomal membrane in response to bacterial infection (Kawahara and Lambeth 2007). On the other hand, autophagy induction by starvation is known to stimulate mitochondrial ROS production (Scherz-Shouval *et al.* 2007; An *et al.* 2020), and Sod2-generated mitochondrial ROS has been shown to be delivered to the bacterial phagosomes during infection (West *et al.* 2011; Abuaita *et al.* 2018). To determine the source of ROS important for the increased lysosomal delivery to the mycobacterial phagosomes during autophagy induction by starvation, we first performed the siRNA-mediated knockdown of Nox2 in RAW264.7 macrophages. Successful knockdown was confirmed by qRT-PCR (Fig. 6A). We then examined the level of ROS associated with mycobacterial phagosomes. RAW264.7 macrophages transfected with siRNAs against Nox2 or scrambled siRNA control were infected with H37Rv or BJN and then induced to undergo autophagy by starvation. ROS associated with mycobacterial phagosomes was detected by DCFDA, as described above. High-content image analysis showed that there was a significant increase in the colocalization of ROS with H37Rv phagosome in the scramble siRNA-transfected RAW264.7 macrophages upon autophagy induction by starvation, while such increase was not observed with the BJN (Fig. 6B and C). In addition, similar results were observed when Nox2-depleted RAW264.7 macrophages were infected with H37Rv or BJN and induced to undergo autophagy by starvation, as seen in the control cells (Fig. 6B and C). These results indicated that the enhanced ROS association with the mycobacterial phagosomes upon autophagy induction by starvation did not depend on Nox2. Moreover, we also examined Cathepsin D colocalization with the mycobacteria in Nox2-deficient RAW264.7 macrophages induced to undergo autophagy by starvation. While a significant increase in Cathepsin D colocalization with H37Rv was observed in the scramble siRNA-transfected RAW264.7 macrophages upon autophagy induction by starvation, such effect was not seen with the BJN (Fig. 6D and E). Similarly, increased Cathepsin D-H37Rv colocalization was also observed in the Nox2-deficient RAW264.7 macrophages induced to undergo autophagy by starvation, but not seen when cells were infected with the BJN (Fig. 6D and E). Altogether, these findings suggested that the enhanced lysosomal delivery to the mycobacterial phagosomes during starvation-induced autophagy did not depend on Nox2.

To determine whether Sod2 plays a role in enhanced ROS association with and lysosomal delivery to mycobacterial phagosomes during autophagy induction by starvation, we depleted Sod2 from RAW264.7 macrophages using siRNA-mediated knockdown. Successful knockdown of Sod2 expression was confirmed by qRT-PCR (Fig. 7A). We then examined the colocalization of different mycobacteria with ROS in the host macrophages. In agreement with our previous results, a significant increase in the colocalization of ROS with H37Rv could be detected in scrambled siRNA-

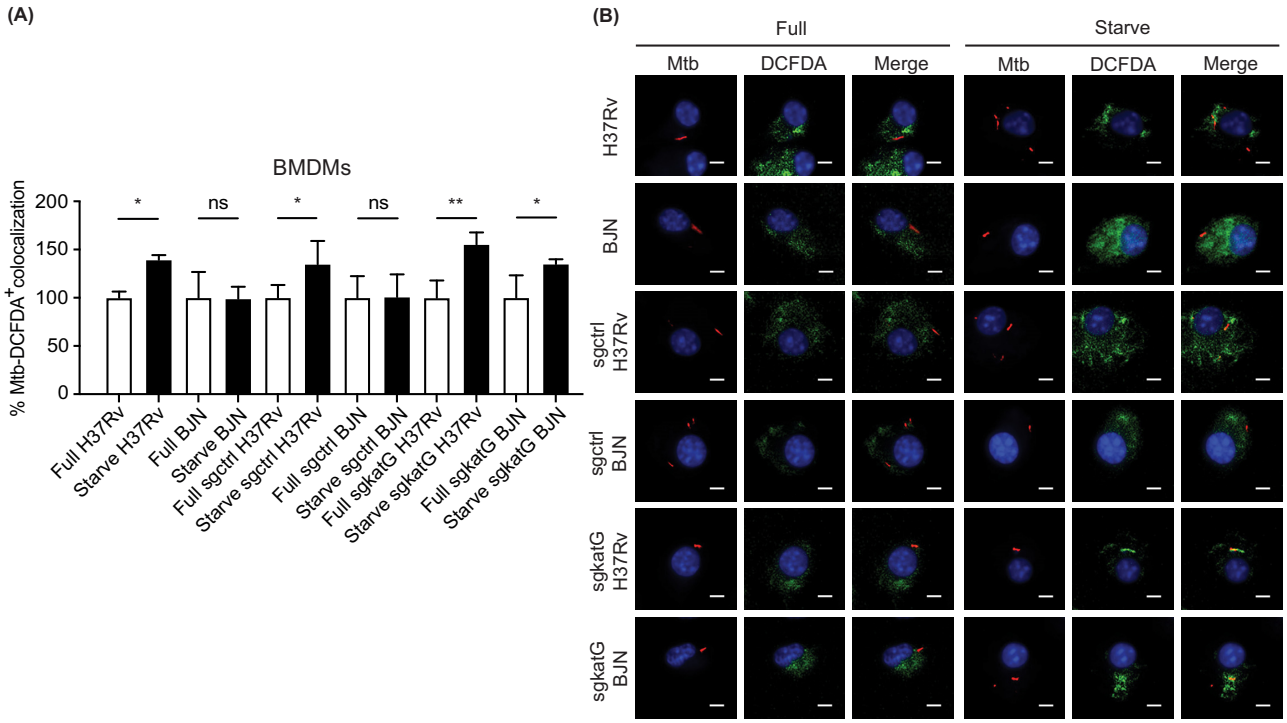

Figure 5. KatG decreases ROS–BJN phagosome colocalization in BMDMs during starvation-induced autophagy. **(A)** and **(B)** BMDMs were infected with Alexa-568-labelled H37Rv or BJN for 15 min, chased for 1 h, and induced to undergo autophagy by starvation for 2 h. Cells were stained for ROS using DCFDA as in Fig. 4. ROS–mycobacteria colocalization was then determined by high-content image analysis. Data comprise means ± SEM from at least three independent experiments; $^{*}P < .05$ and $^{**}P < .01$, all relative to the full control set to 100%, which were determined by one-way ANOVA with Tukey's multiple comparison test (A). Representative images are shown in (B). Bar 5 μm. Full, macrophages without autophagy induction; starve, macrophages with autophagy induction by starvation; sgctrl, non-targeting sgRNA control; and sgkatG, sgRNA targeting *katG*.

transfected RAW264.7 macrophages upon autophagy induction by starvation, though such a rise was not seen with the BJN (Fig. 7B and C). However, a significant enhancement in ROS–H37Rv colocalization was no longer observed upon autophagy induction by starvation when Sod2 was depleted from the host macrophages (Fig. 7B and C). Similar results were observed with Cathepsin D–mycobacteria colocalization, in which an increase in colocalization of Cathepsin D with H37Rv was seen in the scramble siRNA-transfected RAW264.7 macrophages induced to undergo autophagy by starvation; such enhancement was not seen with the BJN (Fig. 7D and E). However, a significant increase in Cathepsin D–H37Rv colocalization could no longer be observed when Sod2-deficient RAW264.7 macrophages were infected with H37Rv and induced to undergo autophagy by starvation (Fig. 7D and E). Thus, these findings suggested that Sod2 plays a crucial role in enhanced ROS association with and lysosomal delivery to mycobacterial phagosomes upon autophagy induction by starvation.

Discussion

Mycobacterium tuberculosis is a successful intracellular bacterium that caused 1.2 million deaths in 2019 (WHO 2020). Approximately 60% of TB cases occur in Asia, in which the Beijing family is found to be the most prevalent genotype (European Concerted Action on New Generation Genetic, Markers, Techniques for the, Epidemiology, and Control of, Tuberculosis 2006; Luo *et al.* 2019). The success of the Beijing family is unclear. However, the Beijing genotype was previously shown to have a greater ability to survive inside host macrophages, causing high bacterial load and greater mortality rates in animal models, with high acid-fast bacilli, smear-positive sputum in human patients (Zhang *et al.* 1999; Dormans *et al.* 2004; Tsenova *et al.* 2005; Hanekom *et al.* 2007; van der Spuy *et al.* 2009; Portevin *et al.* 2011). The molecular mechanisms and factors underlying this increased ability of the Beijing genotype to survive in the host remain unclear. Recently, we reported that the Beijing strains had a previously unrecognized ability to evade elimination by autophagy, an important innate immune mechanism against *M. tuberculosis* in host macrophages (Haque *et al.* 2015). Induction of autophagy by host cell starvation leads to enhanced lysosomal delivery to and restriction of the *M. tuberculosis* reference strain H37Rv (Gutierrez *et al.* 2004; Ponpuak *et al.* 2009, 2010; Pilli *et al.* 2012; Haque *et al.* 2015). In contrast, we found that strains belonging to the *M. tuberculosis* Beijing genotype can resist such starvation-induced autophagic elimination by dampening the lysosomal delivery to its phagosome, but the mycobacterial factors involved remain unknown (Haque *et al.* 2015).

As host cell starvation was known to induce mitochondrial ROS production (Scherz-Shouval *et al.* 2007) and ROS was demonstrated to be required for efficient autophagosome maturation (Xu *et al.* 2014; An *et al.* 2020), we hypothesized that the autophagy-resistant Beijing strain, dubbed BJN, may upregulate the expression of the ROS-inhibitory factor to escape from starvation-induced autophagic restriction. We found that indeed this was the case, in which the BJN upregulated KatG expression during autophagy induction by starvation of host macrophages and KatG was required for the BJN to escape from starvation-induced lysosomal delivery and autophagic restriction (Figs 1–3). In addition, we found that KatG decreased ROS association with the BJN phagosome during starvation-induced autophagy (Figs 4 and 5), and the source of ROS contributing to the starvation-induced lyso-

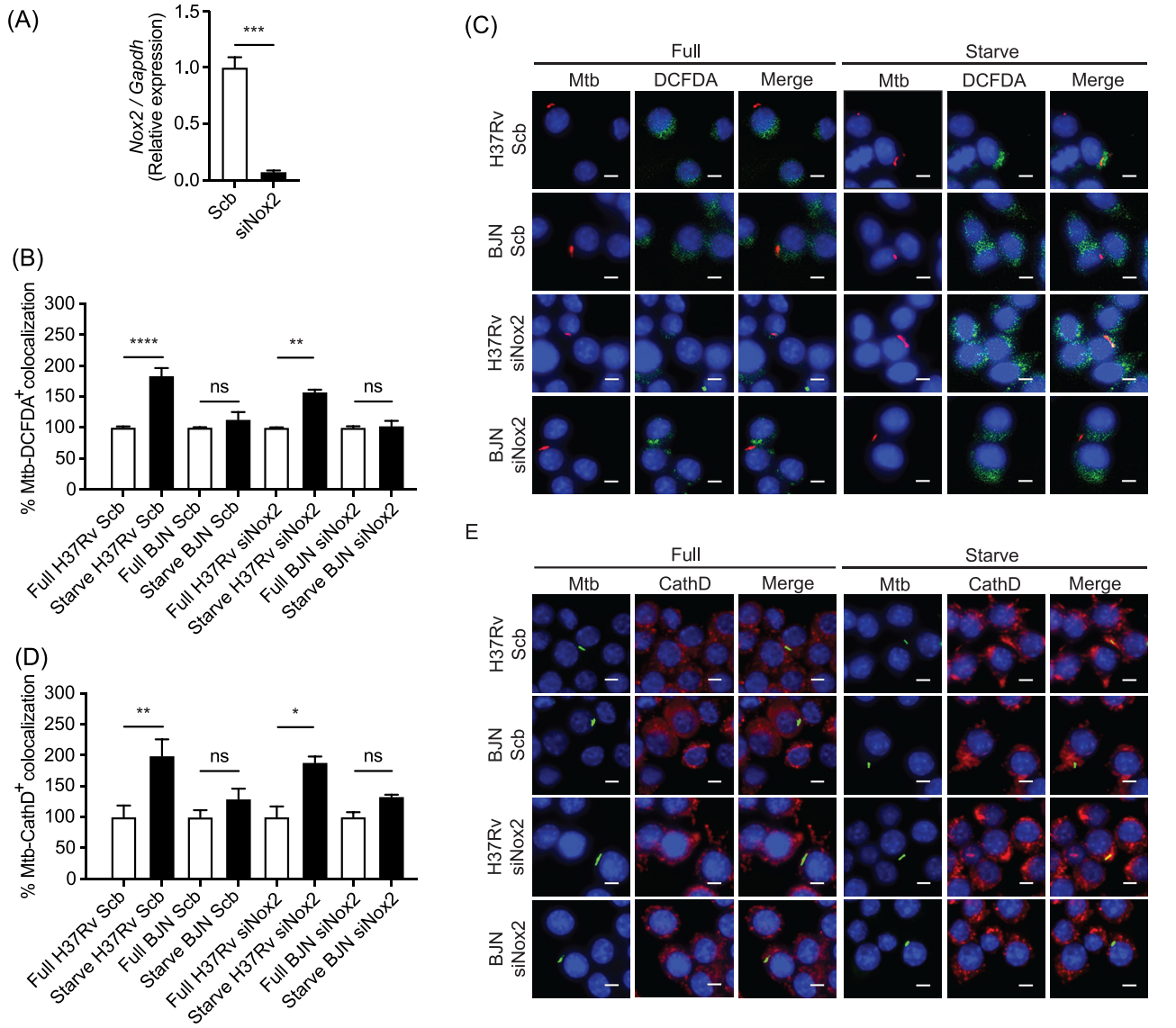

Figure 6. Nox2 is not required for starvation-induced lysosomal delivery to mycobacterial phagosomes. **(A)** RAW264.7 macrophages were transfected with siRNA against Nox2 or scrambled siRNA control. At 48 h after transfection, Nox2 expression was determined by qRT-PCR. Data comprise means ± SEM from at least three independent experiments; ***$P < .001$, relative to scramble siRNA control set to 1.0, which was determined by Student's t-test. **(B)** and **(C)** Nox2-depleted macrophages were infected with the Alexa-568-labelled H37Rv or BJN for 15 min and chased for 1 h. Host cells were then subjected to autophagy induction by starvation for 2 h. ROS was stained with DCFDA for 45 min. Colocalization of ROS with mycobacteria was then analysed by high-content image analysis. Data comprise means ± SEM from at least three independent experiments; **$P < .01$ and ****$P < .0001$, all relative to the full control set to 100%, which were determined by one-way ANOVA with Tukey's multiple comparison test (B). Representative images are shown in (C). **(D)** and **(E)** Nox2-depleted macrophages were infected with the Alexa-488-labelled H37Rv or BJN strain, and then induced to undergo autophagy by starvation, as in (B). Cells were fixed and stained for Cathepsin D. Colocalization of Cathepsin D with mycobacteria was then analysed by high-content image analysis. Data comprise means ± SEM from at least three independent experiments; *$P < .05$ and **$P < .01$, all relative to the full control set to 100%, which were determined by one-way ANOVA with Tukey's multiple comparison test (D). Representative images are shown in (E). Bar 5 μm.

somal delivery to the mycobacterial phagosomes was dependent on Sod2, which generated mitochondrial ROS, but not Nox2, the catalytic subunit of NADPH oxidase (Figs 6 and 7). Altogether, our results identified a new function of KatG in the autophagy evasion by *M. tuberculosis*.

The importance of the autophagy pathway in antimycobacterial defense has been demonstrated substantively and supported by findings that polymorphisms in the autophagy-related genes were found to be associated with susceptibility to tuberculosis (TB; Li *et al.* 2002; Intemann *et al.* 2009; Che *et al.* 2010; King *et al.* 2011; Bahari *et al.* 2012). In addition, mice deficient in Atg5, an important protein required for autophagosome formation in macrophages, display increased susceptibility to mycobacterial infection (Castillo *et al.* 2012; Watson *et al.* 2012). Moreover, a genome-wide siRNA screen to identify host factors that regulate mycobacterial load in macrophages infected with different strains of *M. tuberculosis* revealed autophagy as the main host cell functional module, i.e. perturbed by the pathogen (Kumar *et al.* 2010). However, the mycobacterial factors involved in counteracting autophagy were unknown, until recently. Previous studies showed that the *M. tuberculosis* reference strain H37Rv could inhibit basal autophagy upon infection of host macrophages

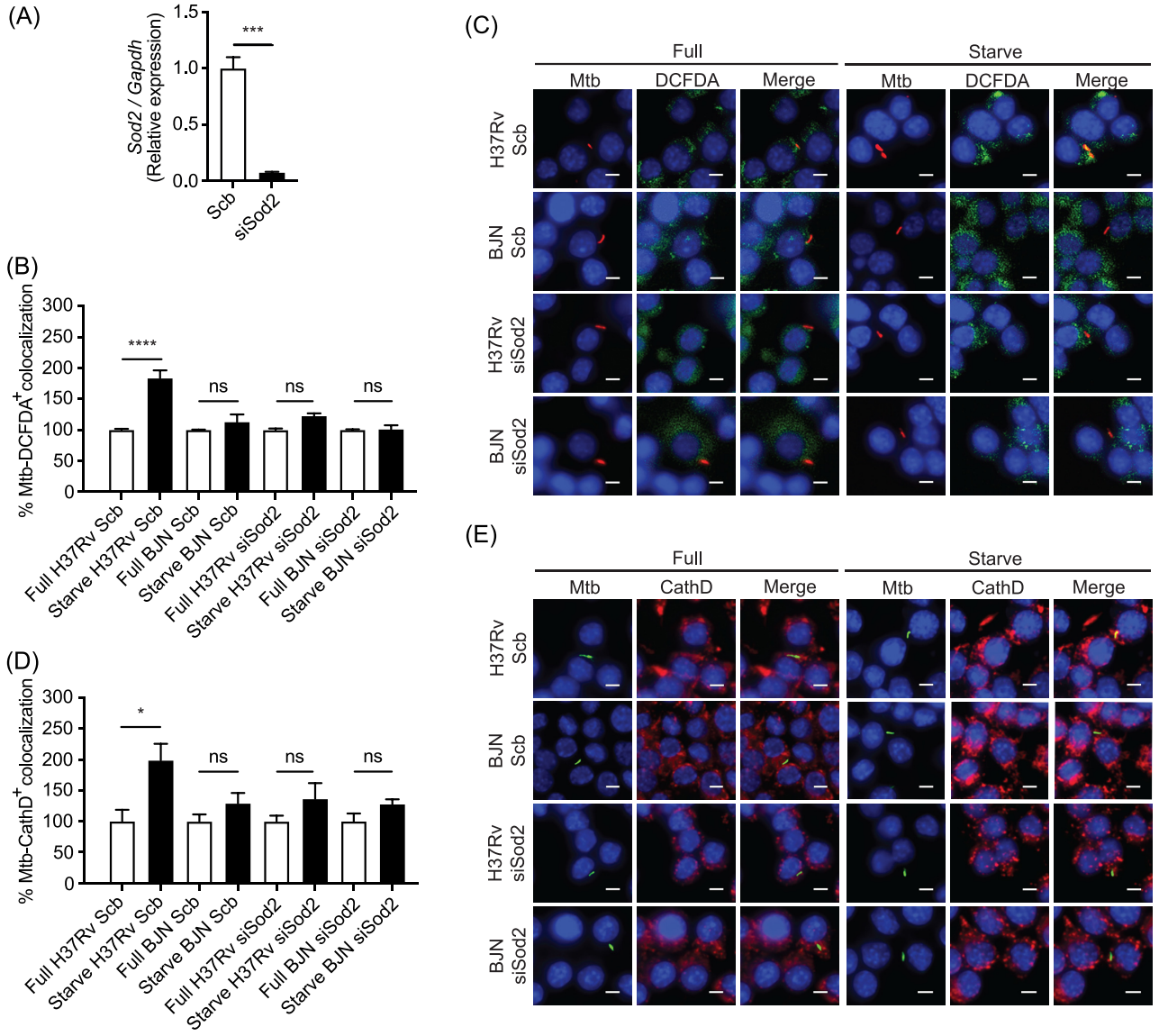

Figure 7. Sod2 is important for enhanced ROS association with and lysosomal delivery to mycobacterial phagosomes during starvation-induced autophagy. (**A**) RAW264.7 macrophages were transfected with siRNAs targeting Sod2 or scrambled control siRNAs. At 48 h after transfection, Sod2 expression was determined by qRT-PCR. Data comprise means ± SEM from at least three independent experiments; ***$P < .001$, relative to the scrambled siRNA control set to 1.0, which was determined by Student's *t*-test. (**B**) and (**C**) Sod2-depleted macrophages were infected with Alexa-568-labelled H37Rv or BJN for 15 min and chased for 1 h. Host cells were then subjected to autophagy induction by starvation for 2 h. Cells were stained for ROS using DCFDA for 45 min and ROS–mycobacteria colocalization was then analysed by high-content image analysis. Data comprise means ± SEM from at least three independent experiments; ****$P < .0001$, relative to the full control set to 100%, which was determined by one-way ANOVA with Tukey's multiple comparison test (B). Representative images are shown in (C). (**D**) and (**E**) Sod2-depleted macrophages were infected with Alexa-488-labelled H37Rv or BJN strain and then induced to undergo autophagy by starvation as in (B). Cells were fixed and stained for Cathepsin D. Colocalization of Cathepsin D with mycobacteria was then analysed by high-content image analysis. Data comprise means ± SEM from at least three independent experiments; *$P < .05$, relative to the full control set to 100%, which was determined by one-way ANOVA with Tukey's multiple comparison test (D). Representative images are shown in (E). Bar 5 μm.

through PE_PGRS47 and Eis proteins, both of which were shown to inhibit autophagosome formation (Shin *et al.* 2010; Saini *et al.* 2016; Strong *et al.* 2021). Under basal autophagy conditions, PE_PGRS47-deficient H37Rv was susceptible to autophagy-mediated elimination, resulting in enhanced autophagy-mediated MHC-II antigen presentation (Saini *et al.* 2016; Strong *et al.* 2021). However, the dampening effect of PE_PGRS47 on the autophagy-mediated MHC-II antigen presentation mentioned above was eliminated when autophagy was induced by rapamycin treatment of host cells (Saini *et al.* 2016), and it was shown that H37Rv could be restricted by rapamycin-induced autophagy (Gutierrez *et al.* 2004). Similarly, macrophages infected with the EIS-deficient H37Rv showed increased autophagosome formation. Further, this enhancement was dependent upon the Nox2-generated ROS (Shin *et al.* 2010). Nevertheless, the enhanced autophagosome formation was Nox2 independent under induced autophagy conditions such as starvation or rapamycin treatment (Shin *et al.* 2010). In addition, our work as well as others substantively demonstrated that H37Rv could be eliminated by starvation-induced autophagy (Gutierrez *et al.* 2004; Harris *et al.* 2009; Ponpuak *et al.* 2010; Singh *et al.* 2010; Castillo *et al.* 2012; Pilli *et al.* 2012; Haque *et al.* 2015; Chauhan *et al.* 2016). As a result, KatG identified by our work appears to mediate

autophagy evasion by *M. tuberculosis* under induced condition, in contrast to PE_PGRS47 and Eis, which can inhibit basal autophagy.

KatG is a catalase–peroxidase that was previously shown to play a role in catabolizing ROS generated by host macrophages and thought to prevent direct oxidative damage to the mycobacteria (Manca *et al*. 1999; Ng *et al*. 2004). There are two main sources of ROS in the host macrophages: NADPH oxidase-generated ROS and mitochondrial ROS (Shekhova 2020). Interestingly, *in vivo* study of KatG-deficient *M. tuberculosis*-infected mice showed that KatG appeared to be important for the survival of mycobacteria 2–4 weeks after infection, which corresponded to the time of macrophage activation, but not during early infection in the first 2 weeks (Ng *et al*. 2004). It was thought that during early infection, other factors might be responsible for the resistance of *M. tuberculosis* to host cell oxidative burst-mediated killing in the inactivated macrophages. Indeed, this was the case as subsequent studies identified CpsA to be required for the evasion of *M. tuberculosis* from NADPH oxidase-mediated killing during early infection (Koster *et al*. 2017). CpsA did so by blocking NADPH oxidase recruitment to the mycobacterial phagosome and CpsA-deficient *M. tuberculosis* was attenuated during early infection in mice (Koster *et al*. 2017). However, both wild-type and CpsA-deficient *M. tuberculosis* were similarly eliminated in IFN-γ-activated macrophages (Koster *et al*. 2017). This suggested that NADPH oxidase-generated ROS played a less important role in the control of *M. tuberculosis* once macrophages were activated and that mitochondrial ROS might take on a more important role. In agreement with this idea, it was shown recently that mice lacking mitofusin 2 required for mitochondrial ROS production were highly susceptible to *M. tuberculosis* infection during 3–6 weeks of infection (Tur *et al*. 2020). In addition, research using activated macrophages infected with the KatG-deficient and KatG-overexpressed H37Rv showed a decreased intracellular survival of the KatG-deficient while KatG-overexpressed H37Rv was able to resist such elimination in the activated macrophages (Manca *et al*. 1999). Altogether, these findings suggested the importance of the role of KatG in antagonizing ROS-mediated *M. tuberculosis* elimination in the activated macrophages, in which the source of ROS is primarily from the mitochondria. Of note, factors that activate macrophages such as IFN-γ or starvation i.e. by a pathogen can also induce autophagy and mitochondrial ROS production, and the activated macrophages utilize autophagy as a defense mechanism to eliminate intracellular bacteria (Scherz-Shouval *et al*. 2007; Weiss and Schaible 2015; Shekhova 2020). Our work, therefore, supported the above notion that KatG dampens Sod2-generated mitochondrial ROS associated with mycobacterial phagosomes and decreases autophagy-mediated lysosomal delivery and mycobacterial restriction during induced autophagy. As starvation was used to induce autophagy in our study, whether similar results would be observed under IFN-γ treatment warrants further investigation. In addition, our work highlighted the importance of mitochondrial ROS in the autophagy-mediated restriction of mycobacteria. Recently, mitochondrial ROS was shown to be delivered together with Sod2 inside the mitochondrial-derived vesicles to *Staphylococcus aureus* phagosomes (Abuaita *et al*. 2018). Whether the same mechanism of mitochondrial ROS delivery occurs during *M. tuberculosis* infection is unknown and should be studied further.

As mentioned above, starvation can increase mitochondrial ROS production and autophagy (Scherz-Shouval *et al*. 2007; Mizushima *et al*. 2011; Deretic *et al*. 2013; Filomeni, De Zio and Cecconi 2014; Weiss and Schaible 2015; Shekhova 2020). These ROS, particularly H_2O_2, can induce autophagic flux by various pathways including activation of AMPK to inhibit mTOR, the key negative regulator of autophagy initiation (Inoki *et al*. 2002; Gwinn *et al*. 2008), inhibition of Atg4 to stabilize LC3-II for autophagosome formation (Scherz-Shouval *et al*. 2007) and activation of dynein to enhance autophagosome maturation (Xu *et al*. 2014; An *et al*. 2020). As our previous work showed that the *M. tuberculosis* Beijing strains could resist starvation-induced autophagic restriction by dampening the xenophagic flux as shown by a marked decrease in the autophagy-mediated lysosomal delivery to its phagosome, but not altering the general autophagic flux of host macrophages as demonstrated by no difference in the number of general autophagosomes and autolysosomes in the infected cells (Haque *et al*. 2015). In addition, by using RNA-Seq analysis of H37Rv- and BJN-infected macrophages, we recently identified host factors, Kxd1 and Plekhm2 which function in lysosome positioning toward the cell periphery, to contribute to autophagy resistance by the BJN (Laopanupong *et al*. 2021). By upregulating the aforementioned host proteins in the infected macrophages, the BJN could promote the lysosome distribution toward the cell periphery and away from its phagosome, thereby sparing itself from autophagy-mediated lysosomal delivery and restriction (Laopanupong *et al*. 2021). As ROS was shown to activate dynein to enhance movement of autophagosomes toward the perinuclear region to fuse with the juxtanuclear lysosomes, resulting in autophagosome maturation (Xu *et al*. 2014). By upregulating KatG, and thus dampening ROS association with its phagosome, whether the BJN could decrease dynein activation and retardation of its phagosome movement to fuse with the juxtanuclear lysosomes warrants further study and was a subject of our investigation.

In addition to KatG, *M. tuberculosis* also expresses other ROS-inhibitory factors including an alkyl hydroperoxide reductase, AhpC, and two superoxide dismutases, SodA and SodC (Manca *et al*. 1999; Dussurget *et al*. 2001; Piddington *et al*. 2001). When the wild-type and AhpC-overexpressed H37Rv were infected into human monocytes and then treated with H_2O_2, no difference in the intracellular survival rate between these two strains was detected (Manca *et al*. 1999). In addition, there was no alteration in the growth rate of AhpC-overexpressed or AhpC-deficient H37Rv in mice when compared to that of the wild-type strain (Heym *et al*. 1997; Springer *et al*. 2001). In the case of SodC, it was shown that the viability of SodC-deficient *M. bovis* BCG in the activated BMDMs was comparable to that of the parental strain (Dussurget *et al*. 2001). Moreover, there was no change in the survival of SodC-deficient H37Rv in guinea pigs when compared to that of the wild-type strain (Dussurget *et al*. 2001). These data suggested the less important roles of AhpC and SodC in the intracellular survival of *M. tuberculosis*. Interestingly, the viability of SodA-attenuated H37Rv was decreased in mice when compared to that of the control strain (Edwards *et al*. 2001). In addition, a markedly increase in macrophage infiltration was observed in the lungs of mice infected with the SodA-attenuated H37Rv, but not in mice infected with the control strain (Edwards *et al*. 2001). Whether SodA may contribute to the autophagy evasion of the BJN strain is of interest and a subject of further investigation.

Nonetheless, our previous findings showed that the BJN upregulated the expression of host proteins to move lysosomes toward the cell periphery to decrease fusion to its phagosome, (Laopanupong *et al*. 2021) and our current study showed that the BJN upregulated KatG to dampen ROS associated with and lysosomal delivery to its phagosome, further demonstrating that the BJN utilizes multiple mechanisms to block autophagy-mediated elimination. Further detailed studies of these mechanisms will not only provide a better understanding of host–*M. tuberculosis* interactions,

but may provide a novel target for drug discovery against this notorious pathogen.

Supplementary data

Supplementary data are available at *FEMSPD* online.

Authors contributions

T.S., P.P., P.K., N.K., A.B., and T.K. conducted the experiments and analysed the data with the help of A.T., T.P., S.B., and P.U.; A.C. provided the autophagy-resistant Beijing strains; M.P. conceived the idea and supervised all research; and T.S. and M.P. wrote the manuscript. All authors revised the manuscript.

Acknowledgments

This research was supported by the Specific League Funds from Mahidol University and the National Research Council of Thailand (NRCT) under the Mid-Career Research Grant (Grant # N41A640157) to M.P. and the Royal Golden Jubilee Ph.D. Program (RGJ-ASEAN Grant # Ph.D./0242/2560) to T.S. Partial support was provided by the Faculty of Science, Mahidol University to M.P. We thank Prof. Sarah Fortune, Harvard T.H. Chan School of Public Health, for providing the CRISPRi plasmid.

Competing interests statement. None declared.

REFERENCES

Abuaita, BH, Schultz, TL, O'Riordan, MX. Mitochondria-derived vesicles deliver antimicrobial reactive oxygen species to control phagosome-localized staphylococcus aureus. *Cell Host Microbe* 2018;**24**:625–36.

Aiewsakun, P, Prombutara, P, Siregar, TSP *et al.* Transcriptional response to the host cell environment of a multidrug-resistant *Mycobacterium tuberculosis* clonal outbreak Beijing strain reveals its pathogenic features. *Sci Rep* 2021;**11**:3199.

An, HK, Chung, KM, Park, H *et al.* CASP9 (caspase 9) is essential for autophagosome maturation through regulation of mitochondrial homeostasis. *Autophagy* 2020;**16**:1598–617.

Bach, H, Papavinasasundaram, KG, Wong, D *et al. Mycobacterium tuberculosis* virulence is mediated by PtpA dephosphorylation of human vacuolar protein sorting 33B. *Cell Host Microbe* 2008;**3**:316–22.

Bahari, G, Hashemi, M, Taheri, M *et al.* Association of IRGM polymorphisms and susceptibility to pulmonary tuberculosis in Zahedan, southeast Iran. *Sci World J* 2012;**2012**:950801.

Castillo, EF, Dekonenko, A, Arko-Mensah, J *et al.* Autophagy protects against active tuberculosis by suppressing bacterial burden and inflammation. *Proc Natl Acad Sci USA* 2012;**109**:E3168–76.

Chauhan, S, Kumar, S, Jain, S *et al.* TRIMs and galectins globally cooperate and TRIM16 and galectin-3 co-direct autophagy in endomembrane damage homeostasis. *Dev Cell* 2016;**39**:13–27.

Che, N, Li, S, Gao, T *et al.* Identification of a novel IRGM promoter single nucleotide polymorphism associated with tuberculosis. *Clin Chim Acta* 2010;**411**:1645–9.

Deretic, V, Levine, B. Autophagy, immunity, and microbial adaptations. *Cell Host Microbe* 2009;**5**:527–49.

Deretic, V, Saitoh, T, Akira, S. Autophagy in infection, inflammation and immunity. *Nat Rev Immunol* 2013;**13**:722–37.

Dormans, J, Burger, M, Aguilar, D *et al.* Correlation of virulence, lung pathology, bacterial load and delayed type hypersensitivity responses after infection with different *Mycobacterium tuberculosis* genotypes in a BALB/c mouse model. *Clin Exp Immunol* 2004;**137**:460–8.

Dussurget, O, Stewart, G, Neyrolles, O *et al.* Role of *Mycobacterium tuberculosis* copper-zinc superoxide dismutase. *Infect Immun* 2001;**69**:529–33.

Edwards, KM, Cynamon, MH, Voladri, RK *et al.* Iron-cofactored superoxide dismutase inhibits host responses to *Mycobacterium tuberculosis*. *Am J Respir Crit Care Med* 2001;**164**:2213–9.

European Concerted Action on New Generation Genetic, Markers, Techniques for the, Epidemiology, and Control of, Tuberculosis. Beijing/W genotype *Mycobacterium tuberculosis* and drug resistance. *Emerg Infect Dis* 2006;**12**:736–43.

Filomeni, G, De Zio, D, Cecconi, F. Oxidative stress and autophagy: the clash between damage and metabolic needs. *Cell Death Differ* 2014;**22**:377–88.

Fratti, RA, Backer, JM, Gruenberg, J *et al.* Role of phosphatidylinositol 3-kinase and rab5 effectors in phagosomal biogenesis and mycobacterial phagosome maturation arrest. *J Cell Biol* 2001;**154**:631–44.

Fratti, RA, Chua, J, Vergne, I *et al. Mycobacterium tuberculosis* glycosylated phosphatidylinositol causes phagosome maturation arrest. *Proc Natl Acad Sci USA* 2003;**100**:5437–42.

Gomes, LC, Dikic, I. Autophagy in antimicrobial immunity. *Mol Cell* 2014;**54**:224–33.

Goude, R, Roberts, DM, Parish, T. Electroporation of mycobacteria. *Methods Mol Biol* 2015;**1285**:117–30.

Gutierrez, MG, Master, SS, Singh, SB *et al.* Autophagy is a defense mechanism inhibiting BCG and *Mycobacterium tuberculosis* survival in infected macrophages. *Cell* 2004;**119**:753–66.

Gwinn, DM, Shackelford, DB, Egan, DF *et al.* AMPK phosphorylation of raptor mediates a metabolic checkpoint. *Mol Cell* 2008;**30**:214–26.

Hanekom, M, van der Spuy, GD, Streicher, E *et al.* A recently evolved sublineage of the *Mycobacterium tuberculosis* Beijing strain family is associated with an increased ability to spread and cause disease. *J Clin Microbiol* 2007;**45**:1483–90.

Haque, MF, Boonhok, R, Prammananan, T *et al.* Resistance to cellular autophagy by *Mycobacterium tuberculosis* Beijing strains. *Innate Immun* 2015;**21**:746–58.

Harris, J, Master, SS, De Haro, SA *et al.* Th1-Th2 polarisation and autophagy in the control of intracellular mycobacteria by macrophages. *Vet Immunol Immunopathol* 2009;**128**:37–43.

Heym, B, Stavropoulos, E, Honoré, N *et al.* Effects of overexpression of the alkyl hydroperoxide reductase AhpC on the virulence and isoniazid resistance of *Mycobacterium tuberculosis*. *Infect Immun* 1997;**65**:1395–401.

Huang, J, Brumell, JH. Bacteria-autophagy interplay: a battle for survival. *Nat Rev Microbiol* 2014;**12**:101–14.

Inoki, K, Li, Y, Zhu, T *et al.* TSC2 is phosphorylated and inhibited by Akt and suppresses mTOR signalling. *Nat Cell Biol* 2002;**4**:648–57.

Intemann, CD, Thye, T, Niemann, S *et al.* Autophagy gene variant IRGM -261T contributes to protection from tuberculosis caused by *Mycobacterium tuberculosis* but not by *M . africanum* strains. *PLoS Pathog* 2009;**5**:e1000577.

Kawahara, T, Lambeth, JD. Molecular evolution of Phox-related regulatory subunits for NADPH oxidase enzymes. *BMC Evol Biol* 2007;**7**:178.

King, KY, Lew, JD, Ha, NP *et al.* Polymorphic allele of human IRGM1 is associated with susceptibility to tuberculosis in African Americans. *PLoS ONE* 2011;**6**:e16317.

Koster, S, Upadhyay, S, Chandra, P *et al. Mycobacterium tuberculosis* is protected from NADPH oxidase and LC3-associated phagocytosis by the LCP protein cpsA. *Proc Natl Acad Sci USA* 2017;**114**:E8711–20.

Kumar, D, Nath, L, Kamal, MA *et al.* Genome-wide analysis of the host intracellular network that regulates survival of *Mycobacterium tuberculosis*. *Cell* 2010;**140**:731–43.

Laopanupong, T, Prombutara, P, Kanjanasirirat, P *et al.* Lysosome repositioning as an autophagy escape mechanism by *Mycobacterium tuberculosis* Beijing strain. *Sci Rep* 2021;**11**:4342.

Li, CM, Campbell, SJ, Kumararatne, DS *et al.* Association of a polymorphism in the P2X7 gene with tuberculosis in a Gambian population. *J Infect Dis* 2002;**186**:1458–62.

Luo, D, Chen, Q, Xiong, S *et al.* Prevalence and molecular characterization of multidrug-resistant *M . tuberculosis* in Jiangxi province, China. *Sci Rep* 2019;**9**:7315.

Manca, C, Paul, S, Barry, CE *et al.* *Mycobacterium tuberculosis* catalase and peroxidase activities and resistance to oxidative killing in human monocytes in vitro. *Infect Immun* 1999;**67**:74–9.

Mehra, A, Zahra, A, Thompson, V *et al.* *Mycobacterium tuberculosis* type VII secreted effector EsxH targets host ESCRT to impair trafficking. *PLoS Pathog* 2013;**9**:e1003734.

Mizushima, N, Yoshimori, T, Ohsumi, Y. The role of atg proteins in autophagosome formation. *Annu Rev Cell Dev Biol* 2011;**27**:107–32.

Ng, VH, Cox, JS, Sousa, AO *et al.* Role of KatG catalase-peroxidase in mycobacterial pathogenesis: countering the phagocyte oxidative burst. *Mol Microbiol* 2004;**52**:1291–302.

Piddington, DL, Fang, FC, Laessig, T *et al.* Cu,Zn superoxide dismutase of *Mycobacterium tuberculosis* contributes to survival in activated macrophages that are generating an oxidative burst. *Infect Immun* 2001;**69**:4980–7.

Pilli, M, Arko-Mensah, J, Ponpuak, M *et al.* TBK-1 promotes autophagy-mediated antimicrobial defense by controlling autophagosome maturation. *Immunity* 2012;**37**:223–34.

Ponpuak, M, Davis, AS, Roberts, EA *et al.* Delivery of cytosolic components by autophagic adaptor protein p62 endows autophagosomes with unique antimicrobial properties. *Immunity* 2010;**32**:329–41.

Ponpuak, M, Delgado, MA, Elmaoued, RA *et al.* Monitoring autophagy during *Mycobacterium tuberculosis* infection. *Methods Enzymol* 2009;**452**:345–61.

Portevin, D, Gagneux, S, Comas, I *et al.* Human macrophage responses to clinical isolates from the *Mycobacterium tuberculosis* complex discriminate between ancient and modern lineages. *PLoS Pathog* 2011;**7**:e1001307.

Rock, JM, Hopkins, FF, Chavez, A *et al.* Programmable transcriptional repression in mycobacteria using an orthogonal CRISPR interference platform. *Nat Microbiol* 2017;**2**:16274.

Saini, NK, Baena, A, Ng, TW *et al.* Suppression of autophagy and antigen presentation by *Mycobacterium tuberculosis* PE_PGRS47. *Nat Microbiol* 2016;**1**:16133.

Scherz-Shouval, R, Shvets, E, Fass, E *et al.* Reactive oxygen species are essential for autophagy and specifically regulate the activity of atg4. *EMBO J* 2007;**26**:1749–60.

Shekhova, E. Mitochondrial reactive oxygen species as major effectors of antimicrobial immunity. *PLoS Pathog* 2020;**16**:e1008470.

Shin, DM, Jeon, BY, Lee, HM *et al.* *Mycobacterium tuberculosis* eis regulates autophagy, inflammation, and cell death through redox-dependent signaling. *PLoS Pathog* 2010;**6**:e1001230.

Singh, SB, Ornatowski, W, Vergne, I *et al.* Human IRGM regulates autophagy and cell-autonomous immunity functions through mitochondria. *Nat Cell Biol* 2010;**12**:1154–65.

Springer, B, Master, S, Sander, S,et al. Silencing of oxidative stress response in *Mycobacterium tuberculosis*: expression patterns of ahpC in virulent and avirulent strains and effect of ahpC inactivation. *Infect Immun* 2001;**69**:5967–73.

Strong, EJ, Ng, TW, Porcelli, SA *et al.* *Mycobacterium tuberculosis* PE_PGRS20 and PE_PGRS47 proteins inhibit autophagy by interaction with rab1A. *mSphere* 2021;**6**:e0054921.

Tsenova, L, Ellison, E, Harbacheuski, R *et al.* Virulence of selected *Mycobacterium tuberculosis* clinical isolates in the rabbit model of meningitis is dependent on phenolic glycolipid produced by the bacilli. *J Infect Dis* 2005;**192**:98–106.

Tur, J, Pereira-Lopes, S, Vico, T *et al.* Mitofusin 2 in macrophages links mitochondrial ROS production, cytokine release, phagocytosis, autophagy, and bactericidal activity. *Cell Rep* 2020;**32**:108079.

van der Spuy, GD, Kremer, K, Ndabambi, SL *et al.* Changing *Mycobacterium tuberculosis* population highlights clade-specific pathogenic characteristics. *Tuberculosis (Edinb)* 2009;**89**:120–5.

Vergne, I, Chua, J, Lee, HH *et al.* Mechanism of phagolysosome biogenesis block by viable *Mycobacterium tuberculosis*. *Proc Natl Acad Sci USA* 2005;**102**:4033–8.

Vergne, I, Fratti, RA, Hill, PJ *et al.* *Mycobacterium tuberculosis* phagosome maturation arrest: mycobacterial phosphatidylinositol analog phosphatidylinositol mannoside stimulates early endosomal fusion. *Mol Biol Cell* 2004;**15**:751–60.

Watson, RO, Manzanillo, PS, Cox, JS. Extracellular *M . tuberculosis* DNA targets bacteria for autophagy by activating the host DNA-sensing pathway. *Cell* 2012;**150**:803–15.

Weischenfeldt, J, Porse, B. Bone marrow-derived macrophages (BMM): isolation and applications. *CSH Protoc* 2008;**2008**:pdb prot5080.

Weiss, G, Schaible, UE. Macrophage defense mechanisms against intracellular bacteria. *Immunol Rev* 2015;**264**:182–203.

West, AP, Brodsky, IE, Rahner, C *et al.* TLR signalling augments macrophage bactericidal activity through mitochondrial ROS. *Nature* 2011;**472**:476–80.

WHO. *Global Tuberculosis Report 2020*. 2020

Xu, M, Li, XX, Chen, Y *et al.* Enhancement of dynein-mediated autophagosome trafficking and autophagy maturation by ROS in mouse coronary arterial myocytes. *J Cell Mol Med* 2014;**18**:2165–75.

Yim, WW, Mizushima, N. Lysosome biology in autophagy. *Cell Discov* 2020;**6**:6.

Zhang, M, Gong, J, Yang, Z *et al.* Enhanced capacity of a widespread strain of *Mycobacterium tuberculosis* to grow in human macrophages. *J Infect Dis* 1999;**179**:1213–7.